



Research article

Use of the improved tug-of-war acupuncture for promoting cartilage repair by inducing macrophage polarization in knee osteoarthritis

Jun Yan^a, Suying Jiang^b, Junjie Ma^a, Xuan Zhou^a, Mei Zhao^a, Jinliang Huang^a, Huimeng Zhu^a, Bingyao Huang^a, Ermei Li^a, Hong Chang^{c,*}

^a Department of Rehabilitation, Shenzhen Hospital of Integrated Traditional Chinese and Western Medicine, Shenzhen, 518104, Guangdong, China

^b Hospital Infection Control Section, Shenzhen Hospital of Integrated Traditional Chinese and Western Medicine, Shenzhen, 518104, Guangdong, China

^c Department of Orthopedics, the First Affiliated Hospital of Guangdong Pharmaceutical University, Guangzhou, 510000, Guangdong, China

ARTICLE INFO

Keywords:

Knee osteoarthritis
Tug of war acupuncture
Macrophage polarization

ABSTRACT

Introduction: Knee osteoarthritis (KOA) is a type of joint disease causing degenerative changes that are challenging to treat. The improved tug-of-war acupuncture (BHZF) can improve joint pain in KOA. However, the associated mechanism has not been validated.

Methods: The KOA rabbit model was established. After the surgery, the improved BHZF was provided as an intervention, and the animals were euthanized after 2 weeks. Histopathological changes in the synovium and cartilage were observed on hematoxylin & eosin staining and Safranin O-Fast Green staining. Synovial fluid and serum samples were collected to assess the presence of cytokines using the enzyme-linked immunosorbent assay. The expression of M1 macrophage (CD86) and M2 macrophage (ARG1) markers in the cartilage and synovium was detected via immunohistochemistry and immunofluorescence assays.

Results: The improved BHZF could reduce KOA-related pain and inhibit joint swelling. Further, it significantly maintained the morphology of articular chondrocytes in KOA and reduced the decomposition of the cartilage matrix. Then, it significantly reduced the expression of CD86-positive cells ($P < 0.05$), and increased the expression of ARG1-positive cells in the cartilage and synovium ($P < 0.05$). Moreover, it significantly decreased the expression of inflammatory factors interleukin (IL)-1 beta and tumor necrosis factor-alpha in the serum and synovial fluid ($P < 0.05$), and significantly increased the expression levels of anti-inflammatory cytokines IL-4 and IL-10 ($P < 0.05$).

Conclusions: The improved BHZF can relieve pain and improve cartilage damage by regulating macrophage polarization in KOA.

1. Introduction

Knee osteoarthritis (KOA) is a type of chronic arthritis characterized by joint pain, deformation, and limited movement, with

* Corresponding author. Department of Orthopedics, the First Affiliated Hospital of Guangdong Pharmaceutical University, No. 19 Nonglin Xia Road, Guangzhou, 510000, Guangdong, China.

E-mail address: chong181@126.com (H. Chang).

<https://doi.org/10.1016/j.heliyon.2024.e25495>

Received 19 June 2023; Received in revised form 8 January 2024; Accepted 29 January 2024

Available online 1 February 2024

2405-8440/Â© 2024 The Authors. Published by Elsevier Ltd. This is an open access article under the CC BY-NC-ND license (<http://creativecommons.org/licenses/by-nc-nd/4.0/>).

degenerative changes and articular cartilage destruction, which are the main pathological manifestations [1,2]. Due to the limited self-healing ability of the articular cartilage, if a lesion develops, its pathological changes are often irreversible, which can have a major impact on the work and life of patients [3]. With the acceleration of the China's population aging process, the incidence rate of KOA has been increasing, and this is significantly associated with heavy economic and social burdens. Macrophages are divided into two phenotypes (classic-activated macrophages [M1] and selective-activated macrophages [M2]) [4]. M1 and M2 can be transformed into each other, which is referred to as polarization. Macrophages can sense changes in the internal environment of the joint fluid [5]. M1 initially produces inflammatory markers (specifically phagocytes), clears damaged tissues or invaders, and then polarizes to M2 to inhibit inflammation and promote bone and cartilage repair [6]. Chronic inflammatory reaction dominated by M1 has a major negative impact on bone and cartilage repair. Meanwhile, M2 macrophages secrete different anti-inflammatory factors, pro-vascular factors, and pro-bone formation factors to inhibit inflammation, regulate osteogenesis and chondrogenesis, and repair bone and cartilage damage [7].

The improved tug-of-war acupuncture (BHZF) is a unique method summarized by Professor Xie Guorong of Hunan University of Traditional Chinese Medicine based on his clinical experience [8]. Scholars used BHZF combined with the pushing and kneading of the patellar bone to treat KOA and achieve good clinical outcomes [9]. The current study used the improved BHZF against KOA. Results showed that this method was more effective than traditional treatment in improving clinical outcomes [10]. However, there is no study on the effect of the modified BHZF on macrophage polarization in KOA treatment. This study further explored the specific mechanism of macrophage polarization by evaluating the effects of BHZF on the pathological structure of the joint tissue and the expression of M1 cytokines interleukin-1 beta (IL-1 β) and tumor necrosis factor-alpha (TNF- α) in the synovial fluid and serum, and CD86 (M1 macrophage marker) and arginase 1 (ARG1, M2 macrophage) in the cartilage and synovium of rabbits with KOA in BHZF-treated KOA.

2. Materials and methods

2.1. Experimental animals

In total, 18 healthy male New Zealand White rabbits aged 6 months were obtained from Guangzhou Mingzhu Bio-technology Co., Ltd., and were divided into three groups. The rabbits were raised in an environment that was ordinary-grade and free of common infectious pathogens. The rabbits were kept in a temperature- and humidity-controlled chamber. They were kept separately in stainless steel cages with 12-h light/dark cycle using an automatic timer. The diet and husbandry were standardized. All rabbits had food and water available during the whole study period. The Ethics Committee of Huateng Biomedical Science Co., Ltd. (HTSW210910) approved this study. After the experiment, the rabbits were euthanized via the intravenous administration of 100 mg/kg of sodium pentobarbital (Sigma-Aldrich, St. Louis, MO, the USA).

2.2. Reagents

The new decalcification solution (quick decalcification) (Servicebio G1107), Safranin O-Fast Green solution for bone tissues (Servicebio G1053), CD86 polyclonal antibody (Abcam ab220188), antiliver arginase antibody (Abcam ab92274), goat antirabbit IgG horseradish peroxidase (Biosharp b1003a), rabbit interleukin-1 beta (IL-1 β) enzyme-linked immunosorbent assay (ELISA) kit (CUSABIO CSB-E06900Rb), rabbit tumor necrosis factor-alpha (TNF- α) ELISA kit (CUSABIO CSB-E06998Rb), rabbit IL-4 ELISA kit (CUSABIO CSB-E06902Rb), and rabbit IL-10 ELISA kit (CUSABIO CSB-E06897Rb) were used. The rabbits received 2 g of papain (Biofroxx 1364gr005) with an electronic balance. Then, 48 mL of normal saline was added, and a 4 % papain solution was prepared. Then, the rabbits received 0.18 g of L-homocysteine (Biofroxx 1206gr025) with an electronic balance. Next, 50 mL of normal saline was added to prepare 0.03 mol/L of homocysteine solution. Finally, the papain solution and L-homocysteine solution were mixed in a 2:1 ratio.

2.3. Grouping and modeling of experimental animal models

In the negative control (NC) group, 6 mL/kg of 0.7 % sodium pentobarbital solution was administered intravenously into the ear margin of the rabbits. After the administration of anesthesia, the hair on the left knee joint of the rabbits was removed with a shaver. After disinfection with alcohol, the knee joint of the rabbits was flexed to approximately 45°. The needle was injected into the intercondylar fossa with the knee eye on the lateral edge of the patellar ligament of the knee joint, which is the needle entry point. If the needle reached the femoral joint surface, it was withdrawn at approximately 2 mm. Next, 0.1 mL of normal saline was injected into the joint cavity with a 1-mL syringe. After the injection, the bleeding point was pressed with a cotton ball, and the left knee joint was bent and stretched to completely absorb and infiltrate the whole joint cavity. Modeling was completed on the 1st, 4th, and 7th days, and a fresh drug solution was prepared on the same day for each modeling. To prevent infection, the principle of sterility was cautiously followed in the preparation and configuration of the molding solution. After the last injection, the rabbits were driven to exercise for 30 min every day. For the rest of the time, they were free in the cage. Samples were taken 14 * 3 days after the first injection.

In the model group (KOA, 14 days), the rabbits were injected with 0.7 % sodium pentobarbital solution at a dose of 6 mL/kg intravenously at the ear margin. After the administration of anesthesia, the hair on the left knee joint of the rabbits was removed with a shaver. After disinfection with alcohol, the knee joint of the rabbits was flexed to approximately 45°. The needle was inserted into the intercondylar fossa with the knee eye on the lateral edge of the patellar ligament of the knee joint, which is the needle entry point. If the needle reached the femoral joint surface, it was withdrawn at approximately 2 mm. Then, 0.1 mL of the mixed solution (4 % papain

solution and L-homocysteine) was injected into the joint cavity with a 1-mL syringe. After the injection, the bleeding point was pressed with a cotton ball. The left knee joint was bent and stretched to completely absorb the solution and infiltrate the whole joint cavity. Modeling was completed on the 1st, 4th, and 7th days, and a fresh drug solution was prepared on the same day for each modeling. To prevent infection, the principle of sterility was strictly followed in the preparation and configuration of the molding solution. After the last injection, the rabbits were driven to exercise for 30 min every day. For the rest of the time, they were free in the cage. On the 14th day after the last injection, the Lequesne MG behavioral score of the knee joint was obtained. If the score was >4, the modeling was successful. Feeding was maintained for 14 * 2 days, and samples were then taken.

In the treatment model group (BHZF + KOA), 6 mL/kg of 0.7 % sodium pentobarbital solution was administered intravenously into the ear margin of the rabbits. After the administration of anesthesia, the hair on the left knee joint of the rabbits was removed with a shaver. After disinfection with alcohol, the knee joint of the rabbit was flexed to approximately 45°. The needle was inserted into the intercondylar fossa with the knee eye on the lateral edge of the patellar ligament of the knee joint, which is the needle entry point (BHZF). If the needle reached the femoral joint surface, it was withdrawn at approximately 2 mm. Then, 0.1 mL of mixed solution (4 % papain solution and L-homocysteine) was injected into the joint cavity with a 1-mL syringe. After the injection, the bleeding point was pressed with a cotton ball, and the left knee joint was bent and stretched to completely absorb the solution and infiltrate the whole joint cavity. Modeling was completed on the 1st, 4th, and 7th days, and a fresh drug solution was prepared on the same day for each modeling. To prevent infection, the principle of sterility was strictly followed in the preparation and configuration of the molding solution. After the last injection, the rabbits were driven to exercise for 30 min every day. For the rest of the time, they were free in the cage. On the 7th day after the last injection, the Lequesne MG behavioral score of the knee joint was obtained and sampled. If the score was >4, the modeling was successful. Then, the improved BHZF method was used for treatment. The surgical method was similar to that used in clinical practice. The selected points were equivalent to the heding point, Zusanli point, and inner and outer knee eye points of the human body. In conventional skin disinfection, a 0.3 × 25-mm filiform needle was used. Then, the needle entered from the upper pole of the patella, and it obliquely stabbed the back of the patella for 5 mm. The needle then entered from the Zusanli point, and it obliquely stabbed the knee joint by 10 mm. Flat toning and flat purging were applied, and the needle handle was held tightly with both hands, with the needle tips facing each other. Then, a 0.4 × 25-mm filiform needle was used. Next, the needle entered from both knee eyes and deeply stabbed the opposite side by 10 mm obliquely. The needle was filled and drained flat, and the hole was shaken if the needle was released. The needles at the abovementioned acupoints were kept for 30 min, and the needles were injected twice for 3 min each time, with flat toning and flat purging. The treatment course was once a day for 10 days. Then, the rabbits were allowed to rest for 3 days before the next treatment course. After two consecutive treatment courses, the materials were taken.

2.4. H&E staining and Safranin O-Fast Green staining

Hematoxylin & eosin (H&E) staining and Safranin O-Fast Green staining were performed according to the manufacturer's instructions. Briefly, the knee articular cartilage of the rabbits was harvested and postfixed with 4 % paraformaldehyde. After demineralization, the knee joint was cut on a paraffin microtome. Then, H&E staining (Servicebio G1076) and Safranin O-Fast Green staining (Servicebio G1053) were performed.

2.5. IHC

Before dewaxing, the tissue sections were placed at room temperature for 60 min or baked in an incubator at 60 °C for 20 min. Tissue sections were placed in xylene (10 min), absolute ethanol (5 min), 95 % ethanol (5 min), 70 % ethanol (5 min), phosphate-buffered saline (PBS; Gibco, Grand Island, the USA) (5 min), and PBS (5 min). Next, 3 % H₂O₂/PBS was used. The sample was then blocked at room temperature for 5–10 min, and washed three times with PBS for 2 min each time. Further, 0.01-M sodium citrate buffer solution (pH 6.0) was used to heat and boil for repair for 10–15 min. After heating, the solution was cooled at room temperature with tap water and was washed with PBS for 5 min. Then, a 5 % BSA blocking solution was added dropwise. Next, the solution was blocked at room temperature for 15 min. Primary antibodies including CD86 and ARG1 (1: 50; Abcam) were added dropwise and left overnight at 4 °C. The sample was washed three times with PBS for 2 min each time. Next, polymerized horseradish peroxidase-labeled anti-rabbit/mouse IgG secondary antibody was added dropwise and incubated for 1 h at room temperature. Then, it was washed three times with PBS for 2 min each time, developed using the diaminobenzidine (DAB) method, counterstained with hematoxylin for 20 s, and washed twice with distilled water for 2 min each time. The slices were placed into 50 %, 70 %, 80 %, 90 %, 95 %, and 100 % ethanol for dehydration for 2 min each time. Finally, they were placed into 100 % xylene for 10 min to achieve transparency. The slices with 50 µl of neutral resin were sealed and stored at room temperature.

2.6. Immunofluorescence assay

The sections of each group were dewaxed to water, autoclaved in saturated sodium citrate buffer (Merck, Darmstadt, Germany) for 2 min, and then cooled to room temperature naturally. They were treated with 3 % hydrogen peroxide for 10 min, washed with PBS (Gibco, Grand Island, the USA), and blocked with 1 % bovine serum albumin (BSA; Sigma-Aldrich; Merck KGaA) for 30 min. Then, they were incubated with diluted primary antibodies against CD86 and ARG1 (1: 50; Abcam) overnight at 4 °C. After washing with PBS, the sections were incubated with diluted fluorescent secondary antibodies (1: 50; Abcam) for 1 h at room temperature. After washing with PBS, they were incubated with a drop of 4',6-diamidino-2-phenylindole (Sigma) for 5 min, and treated with an antifluorescent bursting agent. After sealing, the results were evaluated and photographed using a fluorescence microscope (CX31-P; Olympus; Tokyo; Japan).

The ImageJ software (version 1.46: National Institutes of Health, Bethesda, MD, the USA) was applied to calculate the CD86 and ARG1 positivity rates.

2.7. ELISA

The serum and synovial fluid samples were collected. The IL-1 β , TNF- α , IL-4, and IL-10 expression was measured at an absorbance value of 450 nm according to manufacturer's instruction.

2.8. Evaluation indicators

The Lequesne MG behavioral score: the knee joint and the overall status of the rabbits were assessed every day, and the changes in body weight were recorded. The Lequesne MG behavioral score of the rabbit's knee joint could reflect the severity of knee joint dysfunction in general, and the score was proportional to the severity. If the total score was higher, the knee circumference and thigh circumference based on the knee joint function evaluation were worse. One day before the end of modeling, the peripheral diameter of the knee joint of the rabbits in each group was measured. After anesthetizing the rabbit, the hair on the thighs of the rabbits was removed, and the sample to be measured was straightened. Next, a thin line was wrapped around the thigh with the midpoint of the femur as the center, and the thin line was kept close to the skin without indentation. Next, it was marked, and the length of the thin line was measured as the circumference of the thigh. Knee joint diameter evaluation: One day before the end of the treatment, the knee joint diameter of each rabbit group was measured. After anesthetizing the rabbit, the hair around the knees of the rabbits was shaved, and the sample to be measured was straightened. Next, the vernier caliper was placed on both sides of the knee joint of the rabbits. The caliper was close to the skin on both sides of the knee joint without indentation. The vernier caliper was perpendicular to the plane of the knee joint, and the diameter of the knee joint based on the caliper reading was recorded. H&E staining and Safranin O-Fast Green staining were performed to detect joint pathology. The synovial fluid and serum samples were collected to detect M1-type cytokine IL-1 β and TNF- α using ELISA. The IL-4, IL-10, and M2 cytokine expression was assessed. IHC was used to detect the expression of M1 macrophage (CD86) and M2 macrophage (ARG1) markers in the cartilage and synovium.

2.9. Statistical analysis

The measurement data were expressed as means \pm standard error of the mean. Statistical analyses were performed using the Statistical Package for the Social Sciences software version 22.0 (IBM, Chicago, IL, the USA). The Student's *t*-test was used for group comparison. A *P* value of <0.05 was considered statistically significant.

3. Results

3.1. BHZF reduced pain and inhibited joint swelling in the KOA rabbit model

The KOA rabbit models were constructed and then treated with BHZF. We found that the Lequesne MG behavioral score of the rabbits with KOA increased compared with that of the NC rabbits. The BHZF treatment decreased the Lequesne MG behavioral score of the rabbits with KOA (Fig. 1A). After modeling, the peripheral diameter and the knee joint diameter of the rabbits increased. After the BHZF treatment, the peripheral diameter and the knee joint diameter of the rabbits decreased (Fig. 1B and C).

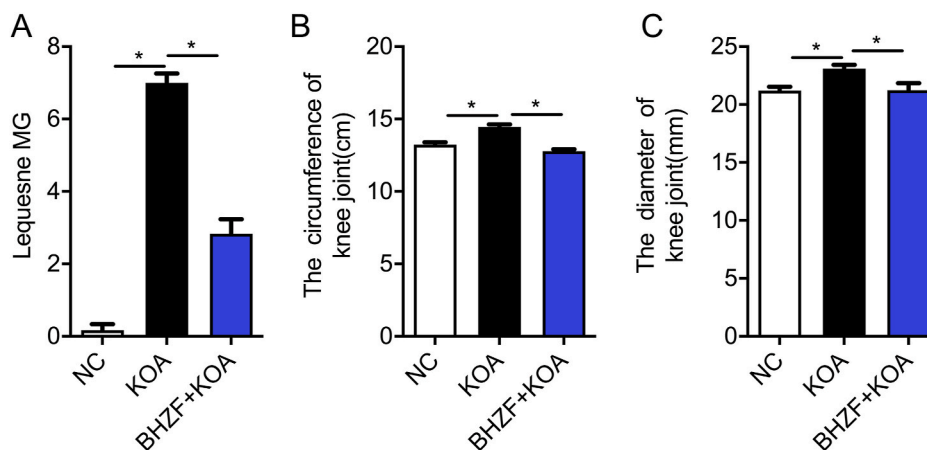


Fig. 1. Effect of BHZF on pain and swelling of KOA model rabbits. The KOA model rabbits were treated with BHZF. (A) The Lequesne MG behavioral score was assessed. (B) The circumference of the knee joint was examined. (C) The diameter of the knee joint was detected. * $P < 0.05$.

3.2. BHZF maintained the morphology of articular chondrocytes and reduced the decomposition of the cartilage matrix in the KOA rabbit model

Subsequently, the pathological structure of the articular cartilage tissue and cartilage matrix was identified on H&E staining and Safranin O-Fast Green staining. H&E staining revealed that the articular cartilage surface of the NC group was basically flat, and the hierarchical structure was clear and complete. Moreover, the chondrocytes were evenly distributed, no clustering was found, and the tide line was clear. In the KOA group, the cartilage surface became thinner and coarser, and it even ruptured with disordered structures and irregular cracks. In the BHZF treatment group, the overall hierarchical structure of the articular cartilage was complete, and the cartilage surface became thin but flat. Moreover, the morphology and size of the chondrocytes were more likely to be normal, and the number slightly increased. A small number of clusters appeared in the shallow layer (Fig. 2A). Safranin O-Fast Green staining results revealed that the cartilage structure of the control group was normal, the cartilage matrix was rich, and Safranin O-Fast Green staining was the most evident. In the KOA group, a large amount of extracellular matrix was decomposed, and safranin staining was significantly reduced compared with the control group. Compared with the KOA group, the cartilage matrix was slightly decomposed, and the degree of safranin staining was slightly increased in the BHZF treatment group (Fig. 2B).

3.3. BHZF reduced the number of CD86-positive cells and increased the number of ARG1-positive cells in the cartilage and synovium in the KOA rabbit model

Based on the IHC results, the number of CD86-positive cells in the bone and synovium of rabbits with KOA significantly increased compared with that in the NC rabbits. After the BHZF treatment, the number of CD86-positive cells significantly decreased in the bone and synovium in the rabbits with KOA (Fig. 3A). Similarly, the number of ARG1-positive cells in the cartilage and synovium of the KOA group significantly increased compared with that in the cartilage and synovium of the NC group. After the BHZF treatment, the number of ARG1-positive cells in the bone and synovium in the KOA rabbit model increased (Fig. 3B). More importantly, the immunofluorescence results also confirmed that BHZF reduced the CD86 expression, which was elevated in the KOA rabbit model (Fig. 3C). Moreover, BHZF also increased the ARG1 expression in the KOA rabbit model (Fig. 3D).

3.4. BHZF reduced the expression levels of inflammatory factors IL-1 β and TNF- α and increased the levels of anti-inflammatory factors IL-4 and IL-10 in the serum and synovial fluid of rabbits with KOA

As shown in Fig. 4A, the expression level of inflammatory factors IL-1 β and TNF- α in the serum of the KOA group was higher than that of the NC group. The IL-4 and IL-10 expression levels increased significantly. After the BHZF treatment, the serum inflammatory factors IL-1 β and TNF- α decreased significantly. However, the expression of anti-inflammatory factors IL-4 and IL-10 continually increased significantly. Fig. 4B depicts that the inflammatory factors IL-1 β and TNF- α in the synovial fluid of the KOA group was higher than that of the NC group. The IL-4 and IL-10 expression levels increased significantly. After the BHZF treatment, the expression levels of inflammatory factors IL-1 β and TNF- α in the synovial fluid decreased significantly. Nevertheless, the expression levels of anti-inflammatory factors IL-4 and IL-10 continually increased significantly.

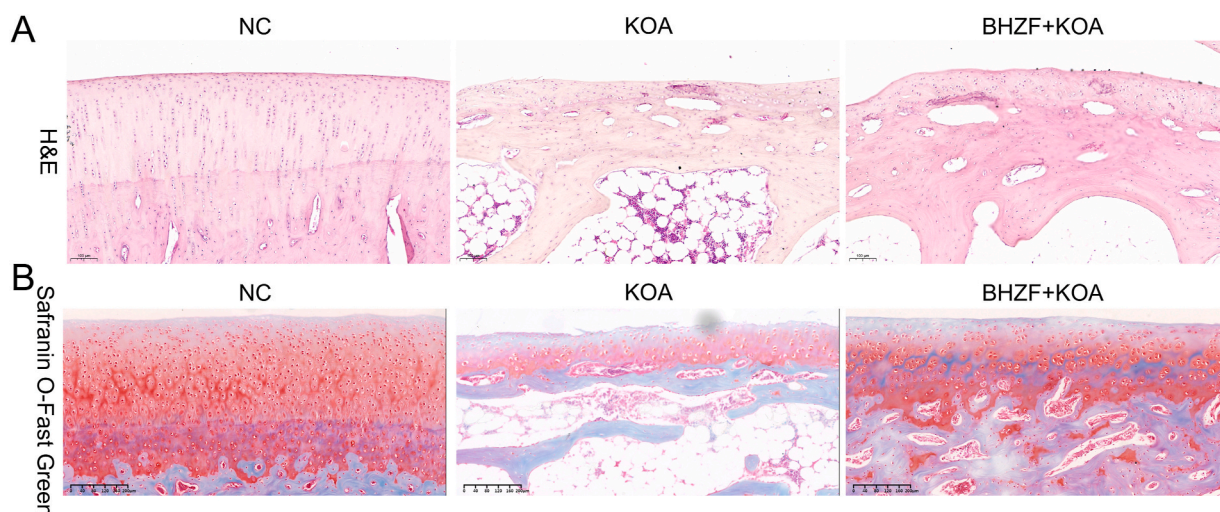


Fig. 2. Effect of BHZF on cartilage recovery of KOA model rabbits. The KOA model rabbits were treated with BHZF. (A) The pathological structure of articular cartilage was assessed by H&E staining. (B) The cartilage matrix was examined using Safranin O-Fast Green staining. (For interpretation of the references to colour in this figure legend, the reader is referred to the Web version of this article.)

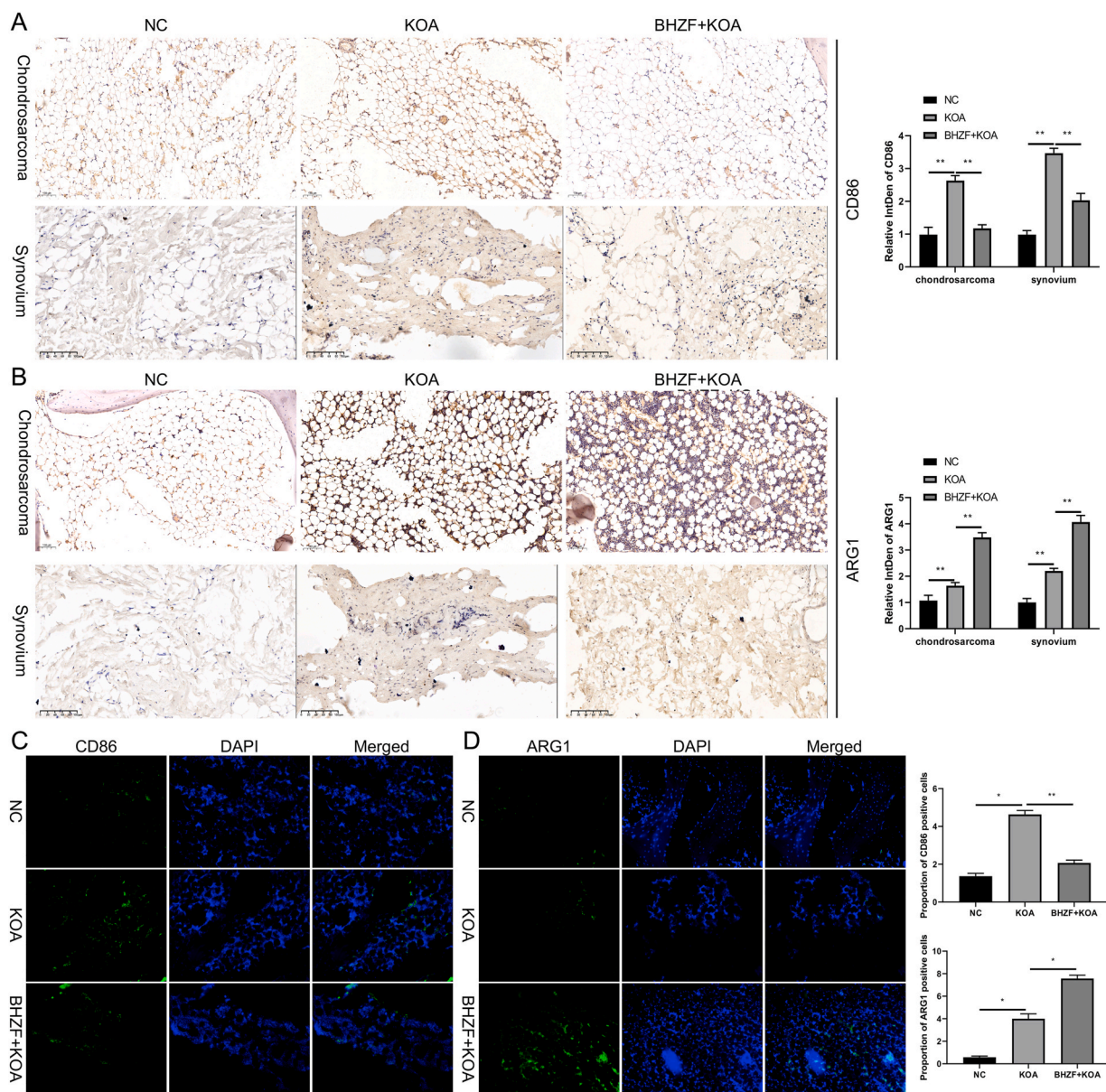


Fig. 3. Effect of BHZF on M1/M2 macrophages in bone and synovium of KOA model rabbits. The number of CD86-positive cells (A) and ARG1-positive cells (B) was detected by IHC assay in bone and synovial tissue of the KOA model rabbits after BHZF treatment. The expressions of CD86 (C) and ARG1 (D) were monitored by IF staining in bone and synovial tissue of the KOA model rabbits after BHZF treatment. * $P < 0.05$, ** $P < 0.01$.

4. Discussion

The knee joint is a joint in the human body that is used to bear weight frequently. It relies on the soft tissue structures (muscles, ligaments, and bursa) around the bone and joint to maintain the stability of the joint and perform daily activities [11]. It is vulnerable to various pathological factors such as rheumatism cold evil and accumulated fatigue injury. The pathological mechanism of KOA is not clear in modern medicine. It is commonly believed that pain, limited movement, and other joint diseases cause degenerative changes inside and outside the knee joint [12]. In traditional Chinese medicine, it has been categorized as arthralgia and bone arthralgia, which commonly occur in patients aged >50 years and those with heavy weight [13]. Traditional Chinese medicine believes that the internal cause of the disease is the gradual decline of kidney qi and the deficiency of liver and kidney essence and blood at approximately 50 years of age [14]. Based on previous studies [8,9], the BHZF method was used for treating KOA (as shown in the grouping and modeling of experimental animal models in the Materials and Methods section). The acupoints selected for this process are the Heding point, Zusanli point, and medial and lateral knee eye points. Among them, the Heding point is located at the top of the knee. Meanwhile, the Zusanli point is located near the knee. Hence, it can relax the tendons and joints and dredge the channels and

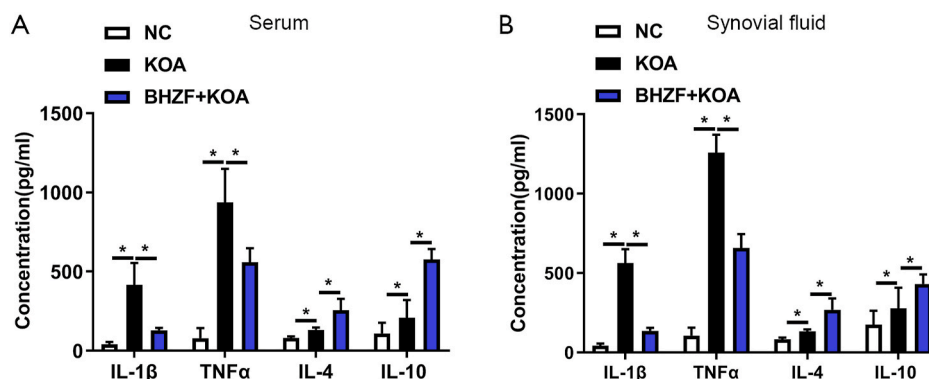


Fig. 4. Effect of BHZF on the expression of key genes and inflammatory factors in KOA model rabbits. (A) After BHZF treatment, the levels of inflammatory factors (IL-1 β and TNF- α) and anti-inflammatory factors (IL-4 and IL-10) were analyzed by ELISA kits in the serum of KOA model rabbits. (B) IL-1 β , TNF- α , IL-4, and IL-10 levels were confirmed using ELISA kits in the synovial fluid of KOA model rabbits after BHZF treatment.

collaterals of the knee [15]. However, during acupuncture and moxibustion integration in the Hedging point, the main two feet are paralyzed and weak. The Zusanli point has a better sense of supporting the right, dispelling evil, and replenishing deficiency. Yangling spring is defined as the meeting of tendons in the difficult scriptures. In addition, according to the compilation of acupoints along the meridians, such as stubborn numbness and cold arthralgia, all thighs, knees, fetuses, and feet are sore and swollen, and it is difficult to move and walk. Matching the two, deficiency can supplement deficiency and strengthen tendons, strengthen knees and bones, and reality can dredge and regulate meridians and tendons, activate collaterals, and relieve pain [16]. The combination of all points has the function of tonifying deficiency and reducing excess, relaxing and benefiting the muscles and bones of the knee, and dredging the blood and blood of the knee. Simultaneously, the penetration needling method in acupuncture can enhance stimulation, can make the acupuncture sense easier to conduct, and have a greater effect, which can significantly relieve knee pain [17]. Our study showed that BHZF could decrease pain (Lequesne MG behavioral score) and joint swelling in the KOA rabbit model. Moreover, it could maintain the morphology of articular chondrocytes and decrease the decomposition of the cartilage matrix. Based on the pathological results, BHZF could also reduce the thickness of the synovium in KOA and the degree of Krenn's pathological grading of synovitis. Therefore, BHZF can be used to treat KOA synovitis.

The development of osteoarthritis is related to different factors. Arthritis plays an important role in the development of osteoarthritis [18]. Different immune cells, including T cells, neutrophils, and macrophages, can regulate inflammation. Macrophages are a highly heterogeneous cell population derived from the bone marrow cell lineage, which exists in almost all tissues and exhibits great anatomical and functional diversity [19]. In recent years, activated macrophages were subdivided into two phenotypes (M1 polarization and M2 polarization). Further, they had opposite inflammatory secretion behaviors, which has attracted significant attention [20]. Macrophage polarization is the most important immune cell in the KOA joint and the most critical cell that regulates the inflammatory state in KOA [21]. Inflammatory factors such as IL-1 β , IL-10, and TNF- α are mainly secreted by macrophages [22]. Considering this finding, previous research has hypothesized that the therapeutic effect of BHZF can be achieved via the following mechanisms: regulating the imbalance of macrophage polarization→affecting the secretion of inflammatory factors→inhibiting intra-articular inflammation→treating synovitis→delaying cartilage degeneration→treating KOA. The current study aimed to validate the effect of the tug-of-war acupuncture on regulating macrophage polarization and inhibiting intra-articular inflammation.

A key aspect of macrophage polarization is the altered expression of cell surface markers [23,24]. CD86 is a molecular marker of M1-type macrophages [25]. M2-type polarization is characterized by a high expression of ARG1, CD206, IL-4, and other factors [26, 27]. Our study confirmed that BHZF could decrease the number of CD86-positive cells and increase the number of ARG1-positive cells in the cartilage and synovium of rabbits with KOA. In addition, previous research showed that M1 macrophages were produced by interferon gamma and lipopolysaccharide induction, thereby upregulating the expression of genes related to pathogen clearance and driving inflammation in response to intracellular pathogens [28]. In contrast, M2 macrophages induced by IL-4 and IL-13 upregulate the expression of genes related to wound healing and participate in anti-inflammatory response [29]. Pro-inflammatory and anti-inflammatory macrophage dysfunction could lead to chronic inflammation and play an important role in chronic inflammatory diseases including osteoarthritis [30]. In our study, based on the ELISA results, BHZF could reduce the levels of inflammatory factors (IL-1 β and TNF- α) and increase the levels of anti-inflammatory factors IL-4 and IL-10 in the serum and synovial fluid of rabbits with KOA. Based on these data, BHZF could inhibit M1-type polarization and promote M2-type polarization to a certain extent in rabbits with KOA. Taken together, this study revealed that BHZF inhibited KOA synovitis by suppressing the secretion of proinflammatory cytokines and by regulating the polarization imbalance of M1/M2 macrophages via the inhibition of M1 polarization.

The current study had some limitations. That is, the sample size was small. Further, Western blot analysis, which is more advantageous than quantitative evaluation, was not performed due to financial constraints. In this experiment, BHZF was found to regulate macrophage polarization to improve the inflammatory environment in KOA to treat the knee joint. Nevertheless, the upstream signal pathway regulating macrophage polarization, nuclear transcription factor, are not been involved- κ B (NF- κ B), mitogen-activated protein kinase (MAPK), a mammalian target protein of rapamycin (mTOR) and related genes, will be the next research

direction.

Theoretically, the degree of inflammation is closely related to the progression of cartilage degeneration, and inhibiting inflammation can effectively improve the degree of cartilage degeneration [31]. However, the experimental results might be attributed to the short treatment time and observation time, which have a specific impact on treatment efficacy. BHZF can improve the secretion of inflammatory factors in animals with KOA mainly by reducing the expression of proinflammatory cytokines. Notably, the IHC results in the cartilage and synovium significantly differed. That is, the cytokines in the cartilage are derived from the penetration of synovial-derived factors and the secretion of chondrocytes themselves. Moreover, the results are primarily affected by the MLS status. Hence, their changes lag behind those in the synovium.

5. Conclusion

BHZF can promote cartilage repair in KOA and improve the treatment effect by inducing macrophage polarization and reducing the release of inflammatory factors, which can be better applied as an optimized treatment method in clinical settings in the future.

Data availability statement

Data will be made available on request.

Funding

This work was funded by Traditional Chinese Medicine Bureau of Guangdong Province, China (20231282); Bao'an TCM Development Foundation (2020KJJCX-KTYJ-140); Sanming Project of Medicine in Shenzhen (SZZYSM202106009).

Ethical statement

This study was approved by the Ethics Committee of the Huateng Biomedical Science Co., Ltd (HTSW210910).

CRediT authorship contribution statement

Jun Yan: Writing – review & editing, Writing – original draft, Methodology, Formal analysis, Data curation, Conceptualization. **Suying Jiang:** Writing – review & editing, Methodology, Investigation, Formal analysis, Data curation, Conceptualization. **Junjie Ma:** Writing – review & editing, Methodology, Investigation, Data curation, Conceptualization. **Xuan Zhou:** Writing – review & editing, Methodology, Investigation, Formal analysis, Data curation, Conceptualization. **Mei Zhao:** Writing – review & editing, Validation, Software, Resources, Data curation, Conceptualization. **Jinliang Huang:** Writing – review & editing, Validation, Software, Resources, Data curation, Conceptualization. **Huimeng Zhu:** Writing – review & editing, Validation, Software, Resources, Data curation, Conceptualization. **Bingyao Huang:** Writing – review & editing, Validation, Software, Resources, Data curation, Conceptualization. **Ermei Li:** Writing – review & editing, Validation, Software, Resources, Methodology, Data curation, Conceptualization. **Hong Chang:** Writing – review & editing, Project administration, Methodology, Investigation, Formal analysis, Data curation, Conceptualization.

Declaration of competing interest

The authors declare that they have no known competing financial interests or personal relationships that could have appeared to influence the work reported in this paper.

Acknowledgements

Not applicable.

References

- [1] L. Zhang, et al., Effect of acupuncture therapies combined with usual medical care on knee osteoarthritis, *J. Tradit. Chin. Med.* 39 (1) (2019) 103–110.
- [2] T. Cheung, et al., Electromoxibustion for knee osteoarthritis in older adults: a pilot randomized controlled trial, *Compl. Ther. Clin. Pract.* 41 (2020) 101254.
- [3] S.G. Atalay, A. Durmus, O. Gezginaslan, The effect of acupuncture and physiotherapy on patients with knee osteoarthritis: a randomized controlled study, *Pain Physician* 24 (3) (2021) E269–E278.
- [4] E. Zajac, et al., Angiogenic capacity of M1- and M2-polarized macrophages is determined by the levels of TIMP-1 complexed with their secreted proMMP-9, *Blood* 122 (25) (2013) 4054–4067.
- [5] J. Cosin-Roger, et al., M2 macrophages activate WNT signaling pathway in epithelial cells: relevance in ulcerative colitis, *PLoS One* 8 (10) (2013) e78128.
- [6] A. Mercalli, et al., Rapamycin unbalances the polarization of human macrophages to M1, *Immunology* 140 (2) (2013) 179–190.
- [7] C.E. Arnold, et al., A critical role for suppressor of cytokine signalling 3 in promoting M1 macrophage activation and function in vitro and in vivo, *Immunology* 141 (1) (2014) 96–110.
- [8] K.Y. Au, et al., Sinew acupuncture for knee osteoarthritis: study protocol for a randomized sham-controlled trial, *BMC Compl. Altern. Med.* 18 (1) (2018) 133.
- [9] R. Plaster, et al., Immediate effects of electroacupuncture and manual acupuncture on pain, mobility and muscle strength in patients with knee osteoarthritis: a randomised controlled trial, *Acupunct. Med.* 32 (3) (2014) 236–241.

- [10] X.J. Yu, et al., Effect of electroacupuncture combined with caudal epidural injection on functional rehabilitation of patients with lumbar hernia, *Zhen Ci Yan Jiu* 46 (7) (2021) 605–609.
- [11] D.E. Huang, et al., Clinical efficacy of different waves of electroacupuncture on knee osteoarthritis and its effect on TGF-beta1 in joint fluid, *Zhongguo Zhen Jiu* 40 (4) (2020) 370–374.
- [12] Y. Zhao, et al., Stiletto needle combined with massotherapy for pain in patients with knee osteoarthritis, *Zhongguo Zhen Jiu* 40 (3) (2020) 247–250.
- [13] Y. Huang, et al., Intra-articular injections of platelet-rich plasma, hyaluronic acid or corticosteroids for knee osteoarthritis : a prospective randomized controlled study, *Orthopä* 48 (3) (2019) 239–247.
- [14] S.Y. Wu, et al., Combined effect of laser acupuncture and electroacupuncture in knee osteoarthritis patients: a protocol for a randomized controlled trial, *Medicine (Baltim.)* 99 (12) (2020) e19541.
- [15] G.X. Shi, et al., Effect of Electro-acupuncture (EA) and manual acupuncture (MA) on markers of inflammation in knee osteoarthritis, *J. Pain Res.* 13 (2020) 2171–2179.
- [16] Z.T. Lv, et al., Effects of intensity of electroacupuncture on chronic pain in patients with knee osteoarthritis: a randomized controlled trial, *Arthritis Res. Ther.* 21 (1) (2019) 120.
- [17] J.F. Tu, et al., Effect of acupuncture on knee injury and osteoarthritis outcome score in patients with knee osteoarthritis, *Zhongguo Zhen Jiu* 41 (1) (2021) 27–30.
- [18] Y. Chen, et al., Comparison of therapeutic effect of different acupuncture methods for knee osteoarthritis, *Zhen Ci Yan Jiu* 45 (7) (2020) 569–573.
- [19] S.Q. Zhuang, et al., Treatment of knee osteoarthritis with acupuncture plus intra-articular injection of sodium Hyaluronate, *Zhen Ci Yan Jiu* 43 (5) (2018) 326–329.
- [20] A. Paoletti, et al., Monocyte/macrophage Abnormalities specific to rheumatoid arthritis are linked to miR-155 and are Differentially Modulated by different TNF Inhibitors, *J. Immunol.* 203 (7) (2019) 1766–1775.
- [21] Y.Y. Huang, et al., Effect of a Novel macrophage-regulating drug on wound healing in patients with diabetic foot ulcers: a randomized clinical trial, *JAMA Netw. Open* 4 (9) (2021) e2122607.
- [22] E.J. Kwak, et al., Chitinase 3-like 1 drives allergic skin inflammation via Th2 immunity and M2 macrophage activation, *Clin. Exp. Allergy* 49 (11) (2019) 1464–1474.
- [23] Y. Zheng, et al., Macrophage-related genes biomarkers in left ventricular remodeling induced by heart failure, *Rev. Cardiovasc. Med.* 23 (3) (2022) 109.
- [24] A. Malone, et al., Regulation of macrophage-associated inflammatory responses by species-specific lactoferricin peptides, *Front. Biosci. (Landmark Ed.)* 27 (2) (2022) 43.
- [25] R. Chen, et al., Overexpression of CD86 enhances the ability of THP-1 macrophages to defend against *Talaromyces marneffe*, *Immun. Inflamm. Dis.* 10 (12) (2022) e740.
- [26] Y. Cheng, et al., Glycyrrhethinic acid suppresses breast cancer metastasis by inhibiting M2-like macrophage polarization via activating JNK1/2 signaling, *Phytomedicine* 114 (2023) 154757.
- [27] L. Li, et al., Sequential gastrin release PU/n-HA composite scaffolds reprogram macrophages for improved osteogenesis and angiogenesis, *Bioact. Mater.* 19 (2023) 24–37.
- [28] J. Rosain, et al., Human IRF1 governs macrophagic IFN- γ immunity to mycobacteria, *Cell* 186 (3) (2023) 621–645.e33.
- [29] S. Montserrat-de la Paz, et al., The effects of exogenous fatty acids and niacin on human monocyte-macrophage plasticity, *Mol. Nutr. Food Res.* 61 (8) (2017).
- [30] C. Liang, et al., Engineered M2a macrophages for the treatment of osteoarthritis, *Front. Immunol.* 13 (2022) 1054938.
- [31] M.L.A. Landsmeer, et al., Predicting knee pain and knee osteoarthritis among overweight women, *J. Am. Board Fam. Med.* 32 (4) (2019) 575–584.